Int. J. Electrochem. Sci., 15 **(2020)** 3761 – 3775, doi: 10.20964/2020.05.14

International Journal of
ELECTROCHEMICAL
SCIENCE
www.electrochemsci.org

Electrochemical Activity of Thin-Film Pd Catalysts Modified with Bi for Methanol and Ethanol Oxidation Reaction in Alkaline Solution

Jelena D. Lović[*], *Sanja I. Stevanović*

ICTM Department of Electrochemistry, University of Belgrade, Njegoševa 12, 11001 Belgrade, Serbia
[*]E-mail: jelena.lovic@ihtm.bg.ac.rs, jlovic@tmf.bg.ac.rs

Received: 6 January 2020 / *Accepted:* 2 March 2020 / *Published:* 10 April 2020

Thin-film Pd catalysts with low metal loadings (55 and 110 μg cm^{-2}) were obtained by electrodeposition from a surfactant-free green electrolyte on glassy carbon (GC) electrode. Pd/GC catalysts were modified by addition of various amounts of Bi via irreversible adsorption. The catalysts were characterized by atomic force microscopy (AFM) and then studied in methanol oxidation reaction (MOR) and ethanol oxidation reaction (EOR) in alkaline solution. Electrochemical tests shown that the modification of the appropriate amount of Bi on Pd/GC catalyst enhance activity toward MOR and EOR up to about 2-3 times compared to unmodified catalysts. Besides surface Bi coverage (Θ_{Bi}) of 0.6 increase durability and provides more poisoning tolerant Pd/GC electrode in both studied reactions. The improvement of electrochemical performances of Bi modified Pd/GC catalysts is attributed to the third body effect and the bifunctional mechanism.

Keywords: Electrodeposition; Palladium; Bismuth adsorption; Alcohol oxidation; Atomic force microscopy.

1. INTRODUCTION

Nanometer-sized particles (NPs) are of increasing importance because of their excellent properties that were noticed in electrocatalysis [1, 2]. Among various noble metal NPs, Pd NPs were successfully applied in electrooxidation of liquid fuels [3, 4], electrochemical sensors [5, 6], hydrogen production and storage [7], pharmaceuticals degradation [8]. The catalytic activity of Pd NPs is determined by their shape, size and surface morphology [2, 9, 10]. In addition, dispersion and high surface area of Pd NPs are substantial factors in creation of high performance Pd-based electrocatalyst [10].

There are numerous research groups that has presented different synthetic methods of nanostructured Pd and Pd based materials. Feasible routes for the creations of Pd NPs imply the reduction

of simple metal salts such as $PdCl_2$ [11]. Besides Pd can be deposited from the bath complexes like H_2PdCl_4, $Pd(NO_3)_2$, $Pd(NH_3)_2(NO_2)_2$, $Pd(NH_3)_2Br_2$ [12]. The other studies were focused on the decomposition of organometallic compounds [13, 14]. Systematical examination of the electrochemical deposition of Pd metallic NPs on Au(111) substrate using an aqueous acidic palladium chloride solution, from the aspect of the applied overpotential and deposition time on nucleation, growth, size and morphology of Pd NPs was presented [15]. The structural characterization of the deposited Pd NPs by means of high-resolution field emission gun-scanning electron microscopy revealed that the electrochemical nucleation occurred randomly on Au substrate and highly dispersed small nuclei or nanoclusters grew independently by the direct reduction of $[PdCl_4]^{-2}$ ions towards the complete coverage of the substrate. Most of the synthetic methods utilize reducing agent, solvent or surfactant in order to control the shape, morphology, dispersity of NPs onto the surfaces of the supports. To avoid demanding experimental conditions such as ultra-high vacuum, several hours of stirring or use of high temperatures, consequently excluding heating or cleaning treatment and presence of organic contaminants in the catalyst, electrodeposition has been demonstrated as promising approach. In particular electrodeposition from a surfactant-free green electrolyte has been in increasing interest [15-17]. The presence of surfactants not only make the synthetic procedure complicated but also release toxic chemicals to the environment. However, electrodeposition from surfactant-free green electrolyte can fulfilled several green chemistry principles (less toxic precursors in water or same environmentally benign solvents, using the least number of reagents and as few synthetic steps as possible also minimising the quantities of generated by-products and waste).

Several studies have dealt with Bi as a plausible Pd surface modifier for the oxidation of alcohols. PdBi/C electrocatalysts with different Pd:Bi atomic ratios were prepared by borohydride reduction method [18]. It was shown that the addition of small quantities of Bi (5 at.%) to Pd/C electrocatalyst enhance the performance for EOR in alkaline medium. PdBi nanowires obtained by thermal decomposition method in the oil phase were tested in methanol and formic acid oxidation [19]. Their results indicated that PdBi NW/XC-72 exhibits better performance for formic acid oxidation than commercial Pd/C but no catalytic activity toward methanol oxidation. PdBi / GC catalyst synthesized by a colloidal route was tested toward the glycerol oxidation reaction as a function of catalyst composition and electrode potential [20]. The Pd0.9Bi0.1/C catalyst displays a higher activity and the onset potential of bimetallic catalyst is shifted by ca. 0.2 V toward lower potentials in comparison with the Pd/C. They concluded that modification of Pd surface by Bi besides the improvement of the activity of glycerol oxidation also affect the composition of chemisorbed species and further the selectivity of catalysts as was proven by High performance liquid chromatography (HPLC) analysis after chronoamperometry experiments at different potentials.

Besides the formation of PdBi alloys using different methods [18-20], one simple way to produce bimetallic surfaces is the irreversible adsorption of adatoms on the Pd surface. When a Pd electrode is immersed into an acidic solution containing Bi_2O_3, a spontaneous adsorption process of Bi^{+3} ions occurs. Considering the adsorption mechanism, it was suggested that the adsorption process of bismuth species on electrode surface occurred via the ionization of adsorbed hydrogen species with subsequent formation of hydroxyl and bismuth adsorbed species [21]. The improvement of the catalytic properties of Pd surfaces caused by the deposition of irreversible adsorbed Bi was found on the oxidation of ethanol [22],

aldehydes [21], glycerol [23]. Cai et al. studied the catalytic activity of Pd/C surfaces modified by irreversible adsorption of Bi in ethanol electrochemical oxidation [22]. Electrochemical measurements show that Pd-Bi/C (20:1) catalyst enhance activity toward ethanol EOR up to about 2.4 times compared to Pd/C catalyst. Besides increased activity, the modification of the appropriate amount of Bi on Pd /C catalyst displays excellent durability and anti-poisoning ability. So far the influence of irreversible adsorption of Bi on Pd in MOR is still missing.

The object of this work is the preparation of Pd/GC catalysts with low metal loadings by electrodeposition from a surfactant-free green electrolyte. The obtained Pd thin-film catalysts were modify via irreversible adsorption of Bi. The catalytic activity and durability of Bi-modified Pd electrodes on methanol and ethanol electro-oxidation in alkaline medium was investigated. The participating roles of Pd and Bi was examined from the aspect of different Pd metal loadings and Bi surface coverages.

2. EXPERIMENTAL

All experiments were carried out with a VoltaLab PGZ 402 (Radiometer Analytical, Lyon, France) at room temperature in three compartment electrochemical glass cells with Pt wire as the counter electrode and saturated calomel electrode (SCE) as the reference electrode. A mirror-like polished GC rotating disk electrode (d = 5 mm) prepared as described elsewhere [24] served as working electrode. All the solutions used were prepared with high-purity UV water (Millipore, 18.2 MΩ cm resistivity) and p.a.-grade chemicals (Merck). The electrolytes were purged with purified nitrogen prior to each experiment.

The palladium electrodeposition on GC electrode was performed from the bath containing 0.05 M $PdCl_2$ + 2 MNH_4Cl at a constant current density of -10 mA cm^{-2} and RPM = 1000 [25]. The electrodeposition process was performed for 10 s and 20 s and the calculated metal loadings were 55 and 110 μg cm^{-2}, respectively. Unmodified Pd electrode with lower metal loading was denoted as Pd-1/GC, while Pd-2/GC corresponded to the electrode that consisted higher metal loading. The Bi modified Pd electrodes were prepared by immersion of the Pd /GC electrode in non-deaerated 0.1 M H_2SO_4 solution containing 10^{-5} M Bi_2O_3 at open circuit potential (ocp) for a certain time. The obtained electrodes were labeled as *x*Bi @)Pd/GC, where *x* refer to Bi surface coverage.

The surface morphology was investigated by AFM with NanoScope 3D (Veeco, USA) microscope operated in taping mode under ambient conditions. Etched silicon probes with spring constant 20 – 80 Nm^{-1} were used. Before morphological examinations of thin-film Pd catalysts, glassy carbon substrate was prepared as previously explained [24]. Image analysis was done by Nanoscope image processing software. The particle diameter of modified and unmodified catalysts was determined from AFM image profile line analysis on the surface area of 2.5 x 2.5 μm^2. Surface roughness (RMS) was determined on the surface area of 10 × 10 μm^2.

3. RESULTS AND DISCUSSION

3.1 Catalyst characterization

The surface morphology studies were based on AFM investigations. Figure 1 demonstrate typical three-dimensional (3D) images of modified and unmodified catalysts on GC surface. AFM image for Pd-1/GC was presented in Fig. 1a. The obtained values of the Pd particles diameter was ~ 90 nm and the structure was composed of spherical shaped agglomerates with uniform size of 185 nm. AFM image for Pd-2/GC catalyst (Fig. 1b) indicated particle diameter ~ 150 nm while the size of agglomerates was ~ 600 nm. Taking into account Bi modified Pd/GC catalysts it can be noticed that particle size increased with Bi coverage and because of that two modified electrodes are chosen for illustration. According to Fig. 1c the estimated particle diameter for Pd-1/GC catalyst modified with Bi for the time of 30 s was ~ 110 nm and the size of agglomerates was ~ 330 nm. Considering Pd-2/GC catalyst when the modification with Bi lasted 60 s, the size of particles was ~ 190 nm without formation of agglomerates.

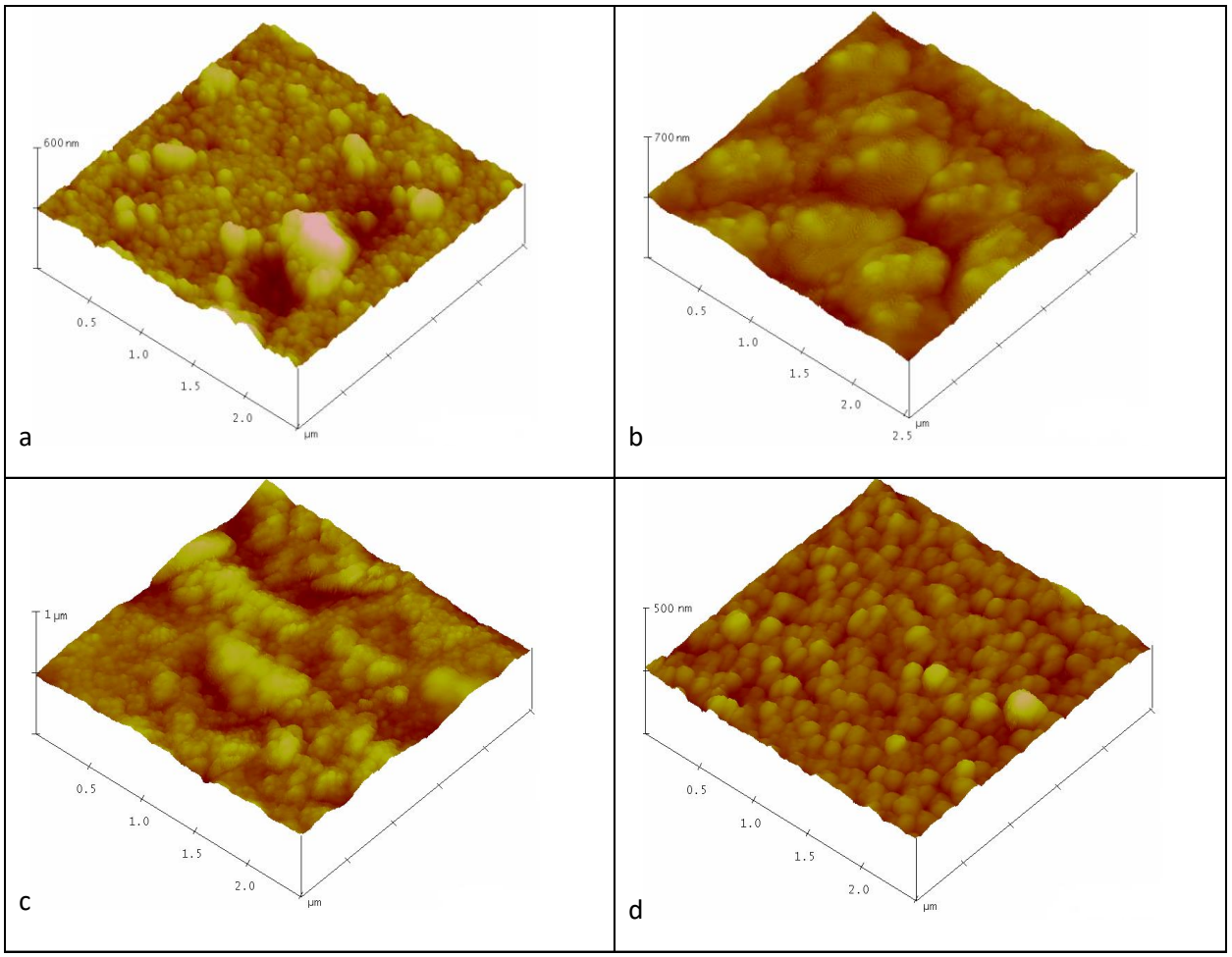

Figure 1. AFM 3D analysis (a) Pd-1/GC (2.5 x 2.5 x 0.6 µm); (b) Pd-2/GC (2.5 x 2.5 x 0.7 µm); (c) Pd-1/GC catalyst modified with Bi for 30 s 2.5 x 2.5 x 1 µm; (d) Pd-2/GC catalyst modified with Bi for the time of 60 s (2.5 x 2.5 x 0.5 µm)

3.2 Electrochemical activity of the catalysts

After the deposition of thin layer of Pd, the modification with Bi at ocp was performed as was described in Experimental section. The resulting electrodes were then rinsed with pure water and transferred to the electrochemical cell containing 0.1 M H_2SO_4 solution for the electrochemical characterization and determination of Bi surface coverage (Fig. 2). The electrochemical response of electrodeposited Pd is in accordance with that obtained at quasi-hemispherical palladium islands onto highly oriented pyrolytic graphite [16]. When Bi is adsorbed on the electrode surface the H adsorption region decreases. The charge involved in the hydrogen desorption process from the Pd surface was determined, and the Bi coverage was calculated [23, 26]. Regarding this electrochemical measurements, for the time of 30 s surface coverage $\theta_{Bi} = 0.2$ was calculated while for duration of 60 s $\theta_{Bi} = 0.6$ was achieved.

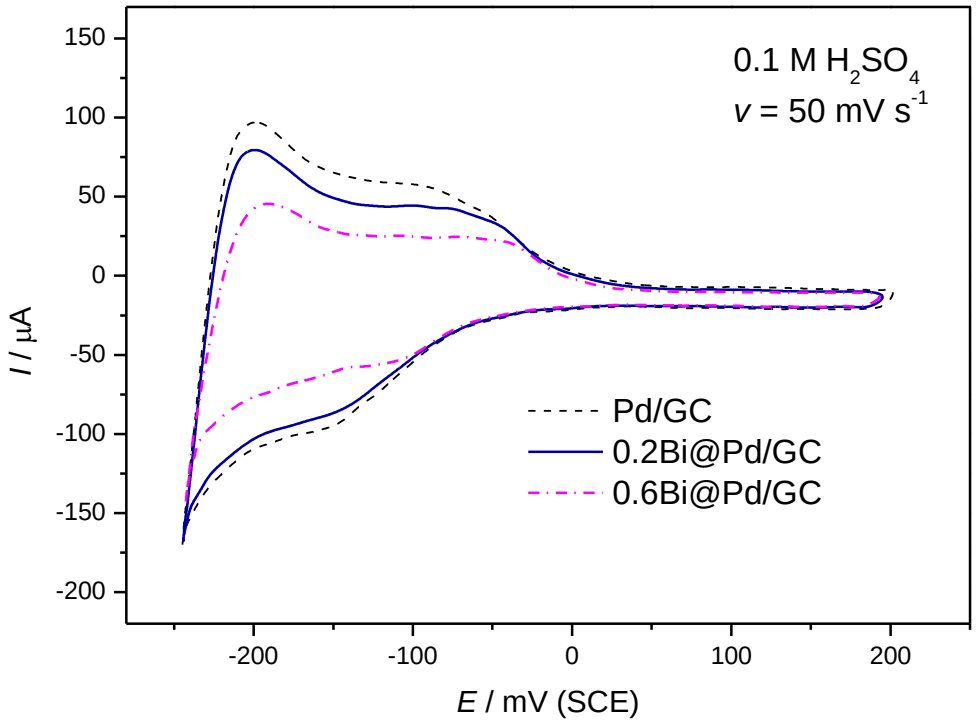

Figure 2. CVs obtained for the Pd/GC catalyst (dash-dot line), 0.2Bi@Pd/GC (solid line) and 0.6Bi@Pd/GC (dash line) in 0.1 M H_2SO_4 at $v = 50$ mV s^{-1}.

The CVs of thin-film Pd and Bi modified Pd electrocatalysts in 1 M NaOH solution at 50 mV s^{-1} were presented in Fig. 3. The behavior of Pd was firstly described and analyzed in order to quantify electrocatalytic activity. Namely, hydrogen adsorption/desorption peaks were shown in the potential range from −1050 to −600 mV [27]. followed by palladium oxide formation region. In the backward scan, palladium oxide was reduced in a broad peak appearing from −200 to −500 mV [28]. The charge under the of peak PdO reduction was used to calculate the electrochemical active surface area (ECSA) value of Pd-based electrocatalysts after subtracting the double layer charge and assuming 420 µC cm^{-2} for the reduction of one monolayer of PdO on the electrocatalyst surface [29, 30]. The calculated ECSA

were given in Table 1. Pd deposits were characterized by the value of specific surface area (SA) in m^2 g_{Pd}^{-1}, as the ratio of electrochemical active surface area and mass of deposited metal (table 1).

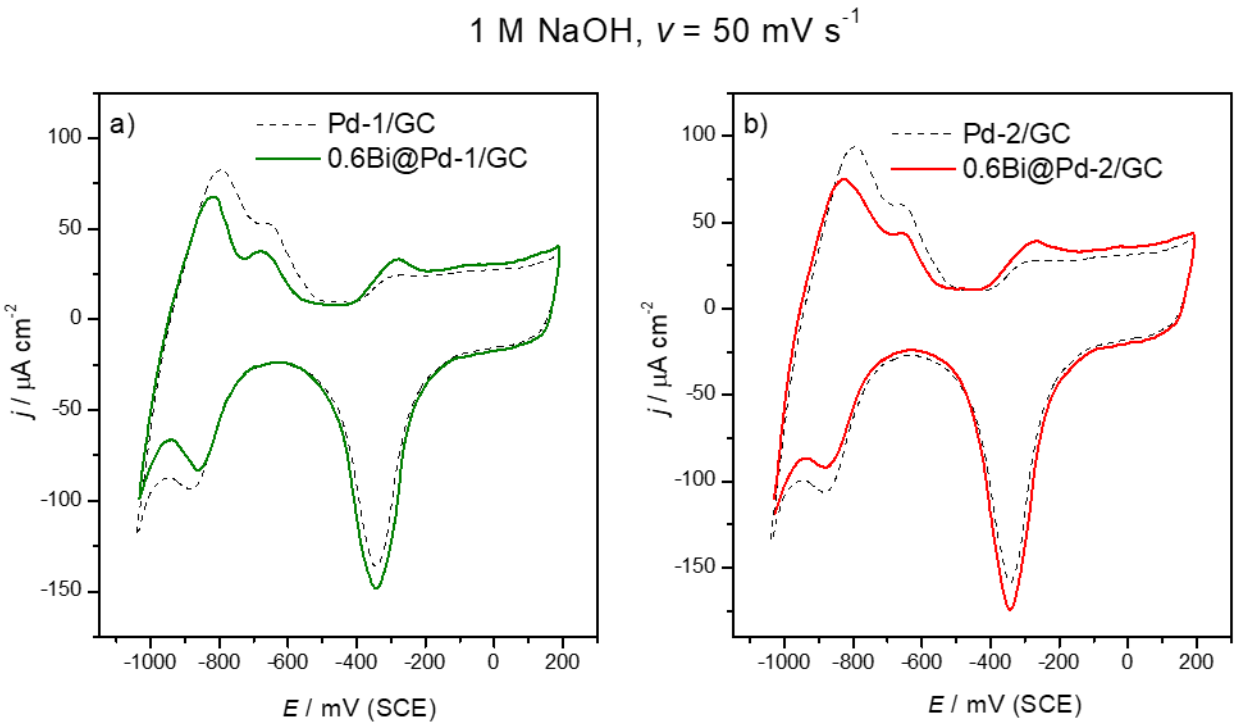

Figure 3. CVs obtained for the Pd/GC catalysts (dash line) and 0.6Bi@Pd/GC (solid line) in 1 M NaOH at v = 50 mV s^{-1}.

Table 1. Parameters that characterize the active surface area of thin-film Pd catalysts

	ECSA / cm²	*mass / µPd*	*SA / m² gPd⁻¹*
Pd-1/GC	0.6	10.8	5.6
Pd-2/GC	0.88	21.6	4.0

In order to estimate the average size of Pd particles in the electrodeposited layer, the next equation was used, assuming that the particles are spherical shape [31, 32].

$$d = \frac{6m_{Pd}}{\rho ECSA}$$

d is the diameter of palladium particles; m_{Pd}, mass of electrodeposited palladium; ρ, density of metallic palladium. The average diameter of Pd particles in the thin layer of catalyst was 95 nm for Pd-1/GC and 138 nm for Pd-2/GC. The obtained values of the Pd particles diameter were in accordance with AFM analysis (Fig. 1a, b). Bera et al. studied the kinetics process and growth mechanism of the electrodeposited Pd nanocrystals (NCs) on stainless steel substrate from aqueous solution of 2 mM $PdCl_2$ + 0.1 M HCl at potential of 0.3 V *vs.* Ag/AgCl at room temperature [33]. The results of this study indicated that the electrodeposition process involved an instantaneous nucleation and subsequent growth and the electrodeposited palladium particles consisted of a number of nanocrytallites according to the SEM analysis. The surface morphology of the electrodeposited Pd particles was uneven on account of

the preferential growth of obtained nanocrystallites in certain crystallographic directions. Also X-ray photoelectron spectroscopy (XPS) study indicated the metallic Pd based on the presence of Pd(3d5/2) and Pd(3d3/2) peaks at binding energy of 335.9 and 341.2 eV, respectively [34].

As it was observed, the adsorbed Bi suppress the hydrogen adsorption region and at more positive potentials a redox couple due to the Bi redox process was noticed (Fig. 3). In the backward scan, a sharp reduction current peak is notable. This peak is attributed to the reduction of the surface oxides, including bismuth oxides [21] formed during the forward scan, suggesting that bismuth redox process in Bi-modified Pd catalyst is related to the palladium redox process [22, 35].

3.3. Electrocatalytic performances of thin-film Pd catalysts modified with Bi in methanol and ethanol oxidation reaction in alkaline solution

The electrocatalytic activity of thin-film Pd catalysts modified with Bi was evaluated by electrooxidation of methanol and ethanol and compared with unmodified Pd/GC electrodes (Figs. 4, 5). The MOR and EOR mechanism on Pd [28, 36] propose that the carbonaceous intermediates can be strongly adsorbed on the Pd surface. During MOR, the intermediates are methanol-dehydrogenization products such as CO_{ad}, while in EOR the intermediates are ethanol-dehydrogenization products such as $(CH_3CO)_{ad}$ [37].

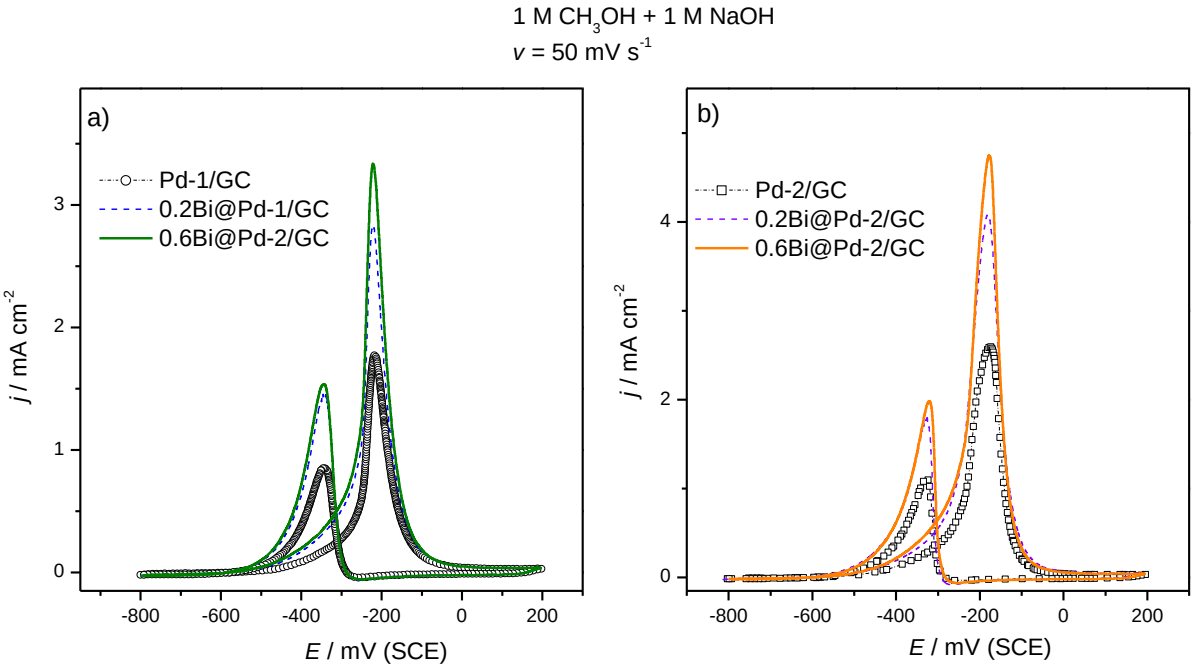

Figure 4. CVs obtained in 1 M CH_3OH + 1 M NaOH with Pd/GC catalysts (dash-dot line), 0.2Bi@Pd/GC (dash line) and 0.6Bi@Pd/GC (solid line) at v = 50 mV s^{-1}.

The Pd begins to adsorb OH^- species in the region of hydrogen adsorption [38], and strongly adsorbed carbonaceous species can be oxidized, causing the increase of current density. The formation of the oxide layer lead to the decrease in the electrocatalytic activity. In the reverse scan the electrode reactivates once the oxide is removed from the Pd surface and reaction currents increase. The peak on

the reverse scan is caused by the oxidation of the incompletely oxidized carbonaceous species, formed during the dissociative adsorption of methanol or ethanol on the Pd in the forward scan [29, 39]. Although the voltammetric profiles were similar, the different onset potentials and peak current values could be attributed to different kinetics of the examined oxidation reactions on Pd/GC. Table 2 summarized the values for the reaction onset potentials as well the ratio of the forward peak current density (j_{pf}) and the backward peak current density (j_{pb}), j_{pf}/j_{pb}, as the parameter of the poisoning tolerance to the carbonaceous species for Pd catalysts. The higher ratio of j_{pf}/j_{pb} imply the more efficient oxidation reaction on the catalyst.

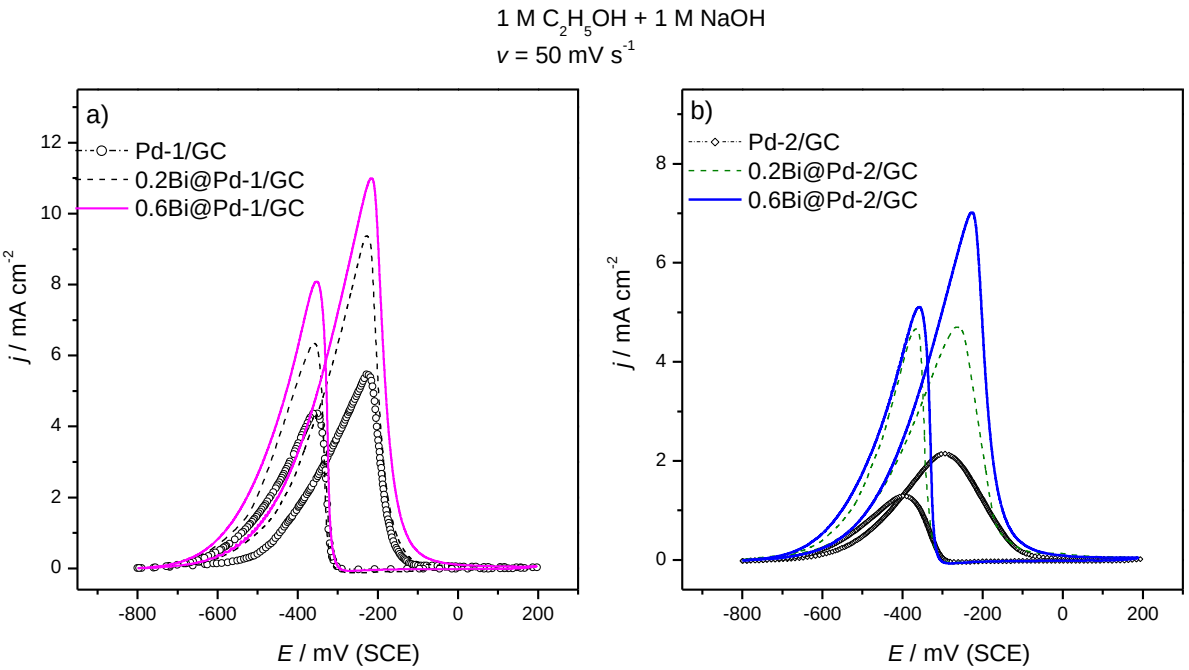

Figure 5. CVs obtained in 1 M C_2H_5OH + 1 M NaOH with Pd/GC catalysts (dash-dot line), 0.2Bi@Pd/GC (dash line) and 0.6Bi@Pd/GC (solid line) at v = 50 mV s^{-1}.

Table 2. Electrochemical data for MOR and EOR

	MOR		*EOR*	
	E_{onset} / mV	j_{pf}/j_{pb}	E_{onset} / mV	j_{pf}/j_{pb}
Pd-1/GC	-500	2	-600	1.3
Pd-2/GC	-500	2.2	-600	1.2
0.2Bi@Pd-1/GC	-550	2.15	-700	1.4
0.6Bi@Pd-1/GC	-550	2.3	-700	1.5
0.2Bi@Pd-2/GC	-550	2.35	-700	1.3
0.6Bi@Pd-2/GC	-550	2.5	-700	1.4

Thin-film Pd catalysts showed higher poisoning tolerance for MOR in regard to the result obtained for EOR implying that the intermediates of methanol oxidation such as CO_{ad} can be oxidized more easily than the intermediates of ethanol oxidation such as $(CH_3CO)_{ad}$. Based on HPLC

measurements, in alkaline solution acetaldehyde tend to form aldol condensation products in small percentage, which might adsorb onto the electrode surface thus blocking it [40]. The present results concerning MOR and EOR obtained on Pd/GC electrodes are consistent with carbon-supported Pd electrocatalyst [41], also with multi-walled carbon nanotube supported Pd nanocatalyst [37]. Thin film Pd catalysts have lower activity towards MOR than EOR, what is in accordance with the reaction mechanism of alcohols oxidation. Namely, the breaking of the α-carbon bonded hydrogen is assumed to be the rate determining step for ethanol oxidation on Pd what was proven by Fourier-transform infrared spectroscopy (FTIR) measurements [42], as well as for methanol oxidation [43]. Since the C-H bond at the α-site in methanol is stronger than in ethanol [44], it is rational to assume that activity towards MOR should be lower than EOR. Therefore from the kinetic point of view MOR is less active than EOR at Pd/GC electrodes in alkaline solution, but the poisoning tolerance of MOR is higher.

According to the results presented in Table 2, the onset potential of Bi modified Pd electrodes was lower than that of the unmodified for 50 mV concerning MOR and 100 mV for EOR. The most active and poisoning tolerant catalyst among studied was 0.6Bi@Pd-2/GC for MOR, while for EOR it was 0.6Bi@Pd-1/GC. The improvement of Bi modified Pd electrode in regard to unmodified Pd can be explained by tree main factors: the change in the electronic properties of the metal substrate, ensemble or third body effect originating from the selective blockage of a particular adsorption site or through bifunctional action [45]. From XPS studies, no matter if Bi was of spontaneously adsorbed or under potential deposited it was concluded that Bi favors the adsorption of OH species, either on its surface or on adjacent noble metal sites [22, 46]. The promotional effect of Bi was obtained on PdBi /C and increased activity was attributed to the enhancement of OH species adsorption on Pd sites adjacent to Bi, which facilitates the oxidative removal of intermediates formed on ethanol electro-oxidation [18]. Cai et al. reveal that the incorporation of Bi into the Pd catalysts modifies the electronic properties of Pd and promotes the formation of oxygen-containing species on Pd surface participating in the oxidation of CO_{ad} according to the bifunctional mechanism, which is beneficial to the enhancement of ethanol electro-oxidation [22]. Bifunctional mechanism of action on PdBi nanostructured thin film was used to explain the enhancement of catalytic properties for ethanol oxidation [47]. In addition, introduction of Bi to tetrahexahedral (THH) Pd NCs increased the activity towards EOR based on electronic effect since the presence of Bi results in a broader and higher current peak in regard to undecorated Pd NCs [26]. In order to determine which of the factor induced by the presence of Bi on the Pd/GC surface influence upon activity of investigated modified electrodes in alcohol oxidation, effect of Bi coverage was studied. According to the obtained results given in Figs. 4, 5, the current densities for MOR and EOR increase with increasing Bi surface coverage. Nevertheless, when higher coverages are reached ($\theta_{Bi} > 0.6$), the currents show a small decrease, being higher than on the unmodified Pd surface. Wang et al. published that with an optimum Bi coverage of 0.68 activity enhancements of almost 3 times were observed for the Bi-modified THH Pd NCs in regard to unmodified THH Pd NCs in ethanol oxidation reaction [26]. Therefore, with high Bi surface coverages a decline of the activity was determined indicating that free Pd atoms are necessary to oxidize methanol or ethanol. It has been proposed that at least three contiguous free Pt sites are required for CO formation [48] and in line with that finding it is reasonable to assume that the irreversible adsorbed Bi plays a third body role diminishing the poisoning of the Pd sites that will then be free for alcohol oxidation. Alongside the enhancement of reaction current densities with

increasing Bi surface coverage, the onset potential of MOR and EOR is independent on Bi surface coverage (Table 2) indicating that a bifunctional catalytic mechanism is valid [49]. The obtained experimental results show that the presence of Bi on the Pd surface stand to two effects for enhancing the alcohol oxidation on Pd/GC. Therefore, the combination of third body and bifunctional effect is responsible for the electrocatalytic improvement of thin-film Pd catalysts modified with Bi in MOR and EOR in alkaline solution.

Figures 6 and 7 show the CVs normalized by the mass of Pd of the unmodified Pd/GC electrodes (Figs 6a and 7a) and of two most active Bi modified electrodes for MOR and EOR (Figs 6b and 7b). Clear differences in terms of peak oxidation currents can be observed comparing the results presented in Figs. 6 and 7. Thus for MOR the difference in j_{pf} between 0.6Bi@Pd-1/GC and 0.6Bi@Pd-2/GC is ~ 15% when the currents were normalized to SA (Fig. 6b) but when the reaction currents were normalized to ECSA enlargement of ~ 2 times in peak current on 0.6Bi@Pd-2/GC in respect to 0.6Bi@Pd-1/GC was noticed (Fig. 4). On the other side taking into account EOR (Fig.7b) the enhancement of ~ 2.2 times on 0.6Bi@Pd-1/GC in respect to 0.6Bi@Pd-2/GC was designated when the currents were normalized to SA or ~ 1.6 times when the reaction currents were normalized to ECSA (Fig. 5). Similar trend in difference of activity concerning peak reaction currents normalized to the total amount of Pd or the electroactive surface area can be notice between unmodified electrodes considering MOR and EOR.

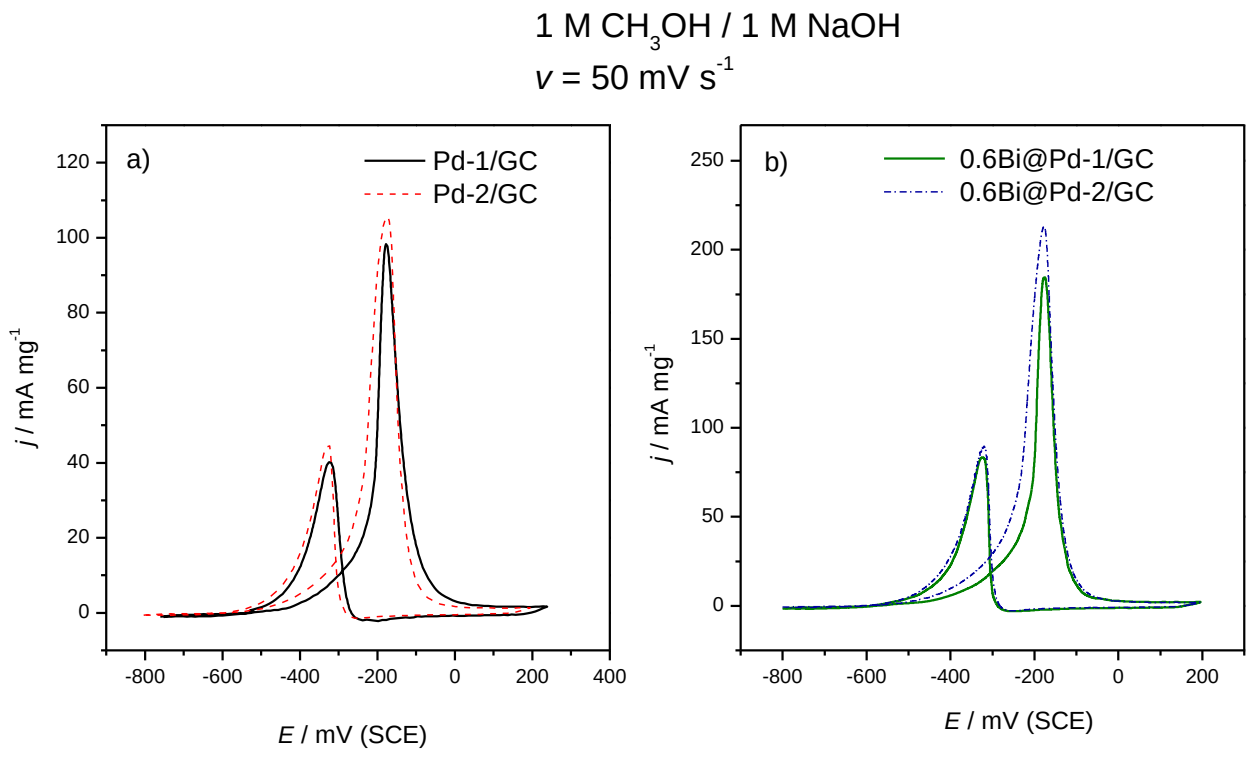

Figure 6. CVs obtained in 1 M NaOH with 1 M CH_3OH on Pd/GC (a) and on 0.6Bi@Pd-1/GC catalysts (solid line) and 0.6Bi@Pd-2/GC (dash line) (b) at v = 50 mV s^{-1}.

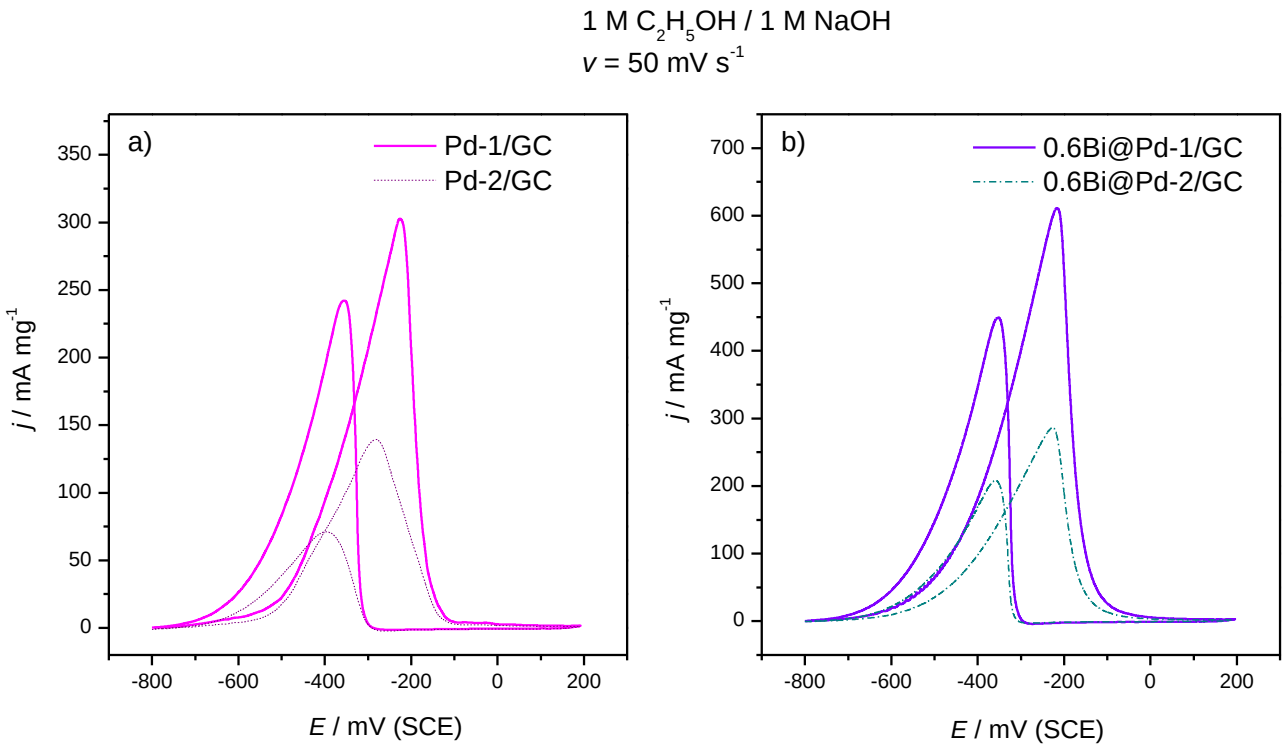

Figure 7. CVs obtained in 1 M NaOH with 1 M C_2H_5OH on Pd/GC (a) and on 0.6Bi@Pd-1/GC catalysts (solid line) and 0.6Bi@Pd-2/GC (dash line) (b) at v = 50 mV s^{-1}.

Comparison of the electrochemical properties from studies of different research groups is sometimes hardly because of different experimental conditions meaning different concentrations of the reactants or supporting electrolyte, various scan rates and rotation rates etc. However, similar activity of MOR and EOR was obtained at Pd supported on highly porous 3D-Graphene nanosheets [50]. Neto et al. reported peak current densities of ~ 60 A g^{-1} for EOR at PdBi / C electrocatalysts, which is lower than in our measurements because of discrepancy in scan rate [18]. Concerning EOR similar peak current density of ~ 8 mA cm^{-2} was obtained on THH Pd NCs modified by Bi adatoms measured in 0.1 M NaOH containing 0.1 M ethanol [26]. Twice larger peak current density compared to our results (~ 1400 A g^{-1}) was reported at ultrathin PdBi nanowires towards ethanol electrooxidation [51] and almost one order of magnitude higher activity on Pd-Bi / C catalyst in regard to this study but at higher ambient temperature which enhances the EOR rate [21]. Other electrochemical properties such as onset potential of the reaction and poisoning tolerance obtained on similar electrocatalysts were collected in Table 3. Analyzing the parameters presented in Tables 2 and 3, it can be concluded that the obtained values are comparable with the published results.

Chronoamperometry was used to study catalysts poisoning in MOR and EOR. The current density - time response of investigated electrodes were recorded at a polarization potential of - 400 mV for 1800 s, as shown in Fig. 8. For all catalysts, there is an initial stage in which the current densities fall rapidly. It should be attributed to the accumulations of poisonous carbonaceous intermediates on the catalyst surface. After that, the currents drop slowly and the electrode reactions reach the pseudo-steady state. It can be notice that most active catalysts in alcohols oxidation showed the highest pseudo-steady

state currents. So the current density of 0.6Bi@Pd-2/GC catalyst in MOR after 1800 s keeps at value which is 5 times higher than that of Pd-2/GC catalyst (Fig. 8b). Regarding EOR, the current density of 0.6Bi@Pd-1/GC catalyst after 1800 s keeps at value which is 3 times higher than that of Pd-1/GC catalyst (Fig. 8c). The catalyst, which exhibits the highest poisoning tolerance and that is 0.6Bi@Pd-2/GC in MOR (Table 2) was also found to be the most stable one in the CA measurements. Apparently addition of Bi enhances the catalytic durability of the Pd/GC catalysts.

Table 3. Electrochemical properties of various catalysts with Bi in MOR and EOR

Catalyst	*Electrolyte*	*Onset potential (mV vs. RHE)*	j_{pf} / j_{pb}	*Reference*
$Pd_{60}Bi_{40}$ / C	1 M KOH + 1 M C_2H_5OH	350 mV	1.7	[52]
THH Pd NCs (Bi = 068)	0.1 M KOH + 0.1 M C_2H_5OH	~ 400 mV	~ 1.5	[26]
PdBi	1 M KOH + 1 M C_2H_5OH	~ 400 mV	1.13	[53]
PtBi NPs	1 M KOH + 1 M CH_3OH	750 mV	7	[54]
Pt_2Bi	1 M KOH + 1 M CH_3OH	~ 700 mV	2	[55]
Pt / ItO (Bi = 0.3)	0.5 M H_2SO_4 + 1 M CH_3OH	~ 560 mV	1.2	[56]

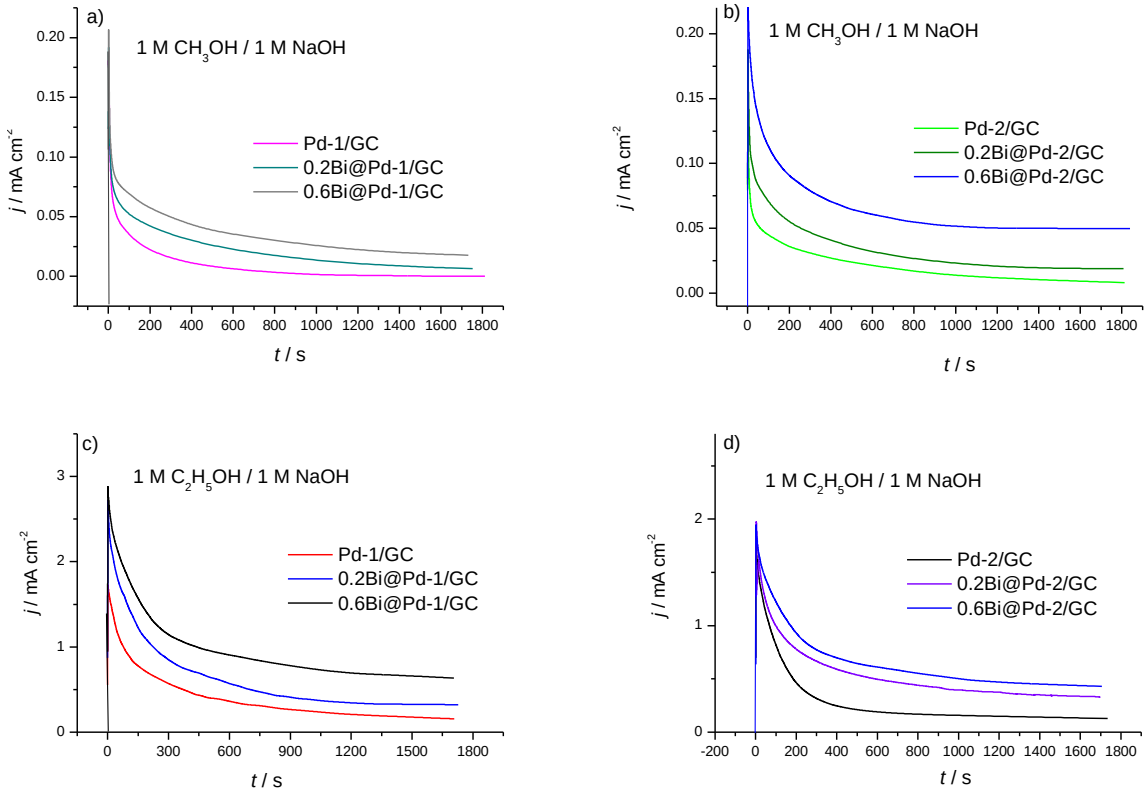

Figure 8. Chronoamperometric curves recorded at - 400 mV (*vs.* SCE) for 1800 s with Pd/GC and *x*Bi@Pd/GC catalysts for methanol (a, b) and ethanol (c, d) in 1 M NaOH.

4. CONCLUSION

Thin-film Pd catalysts with low metal loadings (55 and 110 μg cm^{-2}) were obtained by electrodeposition on CG electrode from a surfactant-free green electrolyte. Surface of Pd electrode is modified by irreversibly adsorbed Bi as fast and easy to do method. The catalysts were characterized by AFM spectroscopy and demonstrated that the nanoparticle clusters was formed from the agglomeration of single crystal particles. The presented electrochemical tests shown that the modification with the appropriate amount of Bi on thin-film Pd catalysts enhance activity toward MOR and EOR up to about 2-3 times compared to unmodified catalysts. Several excellent properties of thin-film Pd catalysts modified with Bi such as high poisoning tolerance and durability were also established. It was concluded that the combination of third body and bifunctional effect is responsible for the electrocatalytic improvement of thin-film Pd catalysts modified with Bi in examined reactions of alcohol oxidation in alkaline solution. Electrochemical investigations of such modified electrodes signify how to direct research in order to develop an efficient catalyst.

ACKNOWLEDGEMENTS
This work was supported by the Ministry of Education, Science and Technological Development of the Republic of Serbia.

References

1. J. M. Campelo, D. Luna, R. Luque, J. M. Marinas, A. A. Romero, *Chem. Sus. Chem.*, 2, (2009) 18.
2. C. Burda, X. Chen, R. Narayanan, M. A. El-Sayed, *Chem. Rev*., 105 (2005) 1025.
3. E. Antolini, E.R. Gonzalez, *J. Power Sources*, 195 (2010) 3431.
4. M. Yusuf, M. Nallal, K. M. Nam, S. Song, S. Park, K. H. Park, *Electrochim. Acta*, 325 (2019) 134938.
5. E Mijowska, M. Onyszko, K. Urbas, M. Aleksandrzak, X. Shi, D. Moszynski, K. Penkala, J. Podolski, M. El Fray, *Appl. Surf. Sci.,* 355 (2015) 587.
6. R. A. Gonçalves, M. R. Baldan, E. G. Ciapina, O. M. Berengue, *Appl. Surf. Sci.,* 491 (2019) 9.
7. S. S. Kumar, V. Himabindu, *Renew. Energy*, 146 (2020) 2281.
8. 8. F. Chen, Q. Yang, D. Wang, F. Yao, Y. Ma, X. Li, J. Wang, L. Jiang, L. Wang, H. Yu, *Chem. Eng. J*., 354 (2018) 983.
9. M. Davi, D. Kesler, A. Slabon, *Thin Solid Films*, 615 (2016) 221.
10. X. Chen, G. Wu, J. Chen, X. Chen, Z. Xie, X. Wang, *J. Am. Chem. Soc*., 133 (2011) 3693.
11. V. D. Jović, U. Č. Lačnjevac, B. M. Jović, Electrodeposition and characterization of alloys and composite materials, in: Djokić S (Eds.) Modern aspects of electrochemistry (2014) Springer, Switzerland.
12. C. R. K. Rao, D.C. Trivedi, *Coordin. Chem. Rev*., 249 (2005) 613.
13. S. Yang, J. Dong, Z. Yao, C. Shen, X. Shi, Y. Tian, S. Lin, X. Zhang, *Sci. Rep*., 4 (2014) 4501.
14. S.-W. Kim, J. Park, Y. Jang, Y. Chung, S. Hwang, T. Hyeon, *Nano Lett*., 3 (2003) 1289.
15. M. Hasan, W. Khunsin, C. K. Mavrokefalos, S. A. Maier, J. F. Rohan, J. S. Foord, *Chem. Electro Chem*., 5 (2018) 619.
16. Y. Gimeno, A. Hernández Creus, S. González, R. C. Salvarezza, A. J. Arvia, *Chem. Mater.*, 13 (2001) 1857.
17. J. Ustarroz, X. Ke, A. Hubin, S. Bals, H. Terryn, *J. Phys. Chem. C*, 116 (2012) 2322.
18. A. Oliveira Neto, M. M. Tusi, N. S. de Oliveira Polanco, S. G. da Silva, M. Coelho dos Santos, E.

V. Spinace, *Int. J. Hydrogen Energy,* 36 (2011) 10522.
19. H. Liao, J. Zhu, Y. Hou, *Nanoscale,* 6 (2014) 1049.
20. M. Simões, S. Baranton, C. Coutanceau, *Appl. Catal. B- Environ*., 110 (2011) 40.
21. I. G. Casella, M, Contursi, *Electrochim. Acta,* 52 (2006) 649.
22. J. Cai, Y. Huang, Y. Guo, *Electrochim. Acta,* 99 (2013) 22.
23. A. Zalineeva, S. Baranton, C. Coutanceau, *Electrochem. Commun*., 34 (2013) 335.
24. J. D. Lovic, S. I. Stevanovic, D.V. Tripkovic, V. M. Jovanovic, R.M. Stevanovic, A.V. Tripkovic, K .Dj. Popovic, *J. Electroanal. Chem*., 735 (2014) 1.
25. J. D. Lović, V. D. Jović, *J. Solid State Electrochem*., 21 (2017) 2433.
26. P. Wang, X. Lin, B. Yang, J.-M. Jin, C. Hardacre, N.-F. Yu, S.-G. Sun, W.-F. Lin, *Electrochim. Acta,* 162 (2015) 290.
27. M. Farsadrooh, J. Torrero, L. Pascual, M. A. Peña, M. Retuerto, S. Rojas, *Appl. Catal. B- Environ*., 237 (2018) 866.
28. Z. X. Liang, T. S. Zhao, J. B. Xu, L. D. Zhu, *Electrochim. Acta,* 54 (2009) 2203.
29. A. Dutta, J. Datta, *J. Mater. Chem. A,* 2 (2014) 3237.
30. J. D. Lovic, N.R. Elezovic, B. M. Jovic, P. Zabinski , Lj. Gajic-Krstajic, V. D. Jovic, *Int. J. Hydrogen Energy,* 43 (2018) 18498.
31. A. A Mikhaylova, O. A Khazova, V. S Bagotzky, *J. Electroanal. Chem*., 480 (2000) 225.
32. T. G. Nikiforova, Yu. V. Kabeneva, O. A. Runova, *Russ. J. Appl. Chem*., 83 (2010) 1001.
33. D. Bera, S. C. Kuiry, S. Seal, *J. Phys. Chem. B,* 108 (2004) 556.
34. J. F. Moulder, W. F. Stickle, P. E. Sobol, K. D. Bomben, Handbook of X-ray Photoelectron Spectroscopy, J. Chastain, Ed.; Physical Electronics Division (1984), Minnesota,USA.
35. A. Zalineeva, A. Serov, M. Padilla, U. Martinez, K. Artyushkova, S. Baranton, C. Coutanceau, P. B. Atanassov, *J. Am. Chem. Soc*., 136 (2014) 3937.
36. M. Zhang, Z. Yan, J. Xie, *Electrochim. Acta,* 77 (2012) 237.
37. W. Chen, Y. Zhang, X. Wei, *Int. J. Hydrogen Energy*, 40 (2015) 1154.
38. M. D. Obradovic, Z. M. Stancic, U. C. Lacnjevac, V.V. Radmilovic, A. Gavrilovic-Wohlmuther, V. R. Radmilovic, S. Lj. Gojkovic, *Appl. Catal. B- Environ*., 189 (2016)110.
39. H. Huang, X. Wang, *J. Mater. Chem*., 22 (2012) 22533.
40. A. Santasalo-Aarnio, Y. Kwon, E. Ahlberg, K. Kontturi, T. Kallio, M. T.M. Koper, *Electrochem. Commun.,* 13 (2011) 466.
41. L. L. Carvalho, F. Colmati, A. A. Tanaka, *Int. J. Hydrogen Energy,* 42 (2017) 16118.
42. J. Ren, Y.-Y. Yang, B.-W. Zhang, N. Tiana, W.-B. Cai, Z.-Y. Zhou, S.-G. Sun, *Electrochem. Commun.,* 37 (2013) 49.
43. Y.-Y. Yang, J. Ren, H.-X. Zhang, Z.-Y. Zhou, S.-G. Sun, W.-B. Cai, *Langmuir,* 29 (2013) 1709.
44. Y. Kwon, S. C. S. Lai, P. Rodriguez, M. T. M. Koper, *J. Am. Chem. Soc.,* 133 (2011) 6914.
45. R. Parsons, T. Vander Noot, *J. Electroanal. Chem*., 257 (1988) 9.
46. U.W. Hamm, D. Kramer, R.S. Zhai, D.M. Kolb, *Electrochim. Acta,* 43 (1998) 2969.
47. N. Xaba, R. M. Modibedi, M. K. Mathe, L.E. Khotseng, *Electrocatalysis,* 10 (2019) 332.
48. A. Cuesta, *J. Am. Chem. Soc*., 128 (2006) 13332.
49. M.C. Figueiredo, R.M. Arán-Ais, J.M. Feliu, K. Kontturi, T. Kallio, *J. Catal*., 312 (2014) 78.
50. A. Serov, N. I. Andersen, S. A. Kabir, A. Roy, T. Asset, M. Chatenet, F. Maillard, P. Atanassov, *J. Electrochem. Soc*., 162 (2015) F1305.
51. X.-T. Zhang, L.-N. Zhou, Y.-Y. Shen, H.-T. Liu, Y.-J. Li, *RSC Adv*., 6 (2016) 58336.
52. B. Cermenek, J. Ranninger, B. Feketeföldi, I. Letofsky-Papst, N. Kienzl, B. Bitschnau, V. Hacker, *Nano Res.,* 12 (2019) 683.
53. X. Yuan, Y. Zhang, M. Cao, T. Zhou, X. Jiang, J. Chen, F.Lyu, Y. Xu, J. Luo, Q. Zhang, Y. Yin, *Nano Lett*., 19 (2019) 4752.
54. M. Yang, *J. Power Sources*, 229 (2013) 42.

55. X. Yuan, X. Jiang, M. Cao, L. Chen, K. Nie, Y. Zhang, Y. Xu, X. Sun, Y. Li, Q. Zhang, *Nano Res.*, 12 (2019) 429.
56. Y. Du, C. Wang, *Mater. Chem. Phys.*, 113 (2009) 927.